Suppressors of amyloid-β toxicity improve recombinant protein production in yeast by reducing oxidative stress and tuning cellular metabolism

Downloaded from: https://research.chalmers.se, 2024-04-26 16:01 UTC

Citation for the original published paper (version of record):
Chen, X., Li, X., Ji, B. et al (2022). Suppressors of amyloid-β toxicity improve recombinant protein production in yeast by reducing
oxidative stress and tuning cellular metabolism. Metabolic Engineering, 72: 311-324.
http://dx.doi.org/10.1016/j.ymben.2022.04.005

N.B. When citing this work, cite the original published paper.

research.chalmers.se offers the possibility of retrieving research publications produced at Chalmers University of Technology.
It covers all kind of research output: articles, dissertations, conference papers, reports etc. since 2004.
research.chalmers.se is administrated and maintained by Chalmers Library

(article starts on next page)

Metabolic Engineering 72 (2022) 311–324

Contents lists available at ScienceDirect

Metabolic Engineering

journal homepage: www.elsevier.com/locate/meteng

Suppressors of amyloid-β toxicity improve recombinant protein production in yeast by reducing oxidative stress and tuning cellular metabolism

Xin Chen [a,b,*], Xiaowei Li [a], Boyang Ji [a,c], Yanyan Wang [a], Olena P. Ishchuk [a], Egor Vorontsov [d], Dina Petranovic [a,b], Verena Siewers [a,b,**], Martin K.M. Engqvist [a]

[a] Division of Systems and Synthetic Biology, Department of Biology and Biological Engineering, Chalmers University of Technology, SE-412 96, Gothenburg, Sweden
[b] Novo Nordisk Foundation Center for Biosustainability, Chalmers University of Technology, SE-412 96, Gothenburg, Sweden
[c] BioInnovation Institute, Ole Måløes Vej 3, DK-2200, Copenhagen N, Denmark
[d] Proteomics Core Facility, Sahlgrenska Academy, University of Gothenburg, SE-413 90, Gothenburg, Sweden

ARTICLE INFO

Keywords:
Amyloid-β
Protein misfolding and aggregation
Cell stress
Yeast cell factories
Cell engineering

ABSTRACT

High-level production of recombinant proteins in industrial microorganisms is often limited by the formation of misfolded proteins or protein aggregates, which consequently induce cellular stress responses. We hypothesized that in a yeast Alzheimer's disease (AD) model overexpression of amyloid-β peptides (Aβ42), one of the main peptides relevant for AD pathologies, induces similar phenotypes of cellular stress. Using this humanized AD model, we previously identified suppressors of Aβ42 cytotoxicity. Here we hypothesize that these suppressors could be used as metabolic engineering targets to alleviate cellular stress and improve recombinant protein production in the yeast *Saccharomyces cerevisiae*. Forty-six candidate genes were individually deleted and twenty were individually overexpressed. The positive targets that increased recombinant α-amylase production were further combined leading to an 18.7-fold increased recombinant protein production. These target genes are involved in multiple cellular networks including RNA processing, transcription, ER-mitochondrial complex, and protein unfolding. By using transcriptomics and proteomics analyses, combined with reverse metabolic engineering, we showed that reduced oxidative stress, increased membrane lipid biosynthesis and repressed arginine and sulfur amino acid biosynthesis are significant pathways for increased recombinant protein production. Our findings provide new insights towards developing synthetic yeast cell factories for biosynthesis of valuable proteins.

1. Introduction

Recombinant proteins underpin important breakthroughs in biomedical biotechnology, resulting in advances for treating diseases from anemia to cancer (Pham, 2018). Since human insulin was first produced in 1982 (Johnson, 1982), recombinant protein engineering has dramatically evolved, and more than 170 recombinant proteins are produced and used in medical fields (Walsh, 2018). Microorganisms as well as cultured cells from other organisms (mammalian, insect, and plant) are the most common expression platforms for recombinant protein production (Tripathi and Shrivastava, 2019). Among them, yeast *Saccharomyces cerevisiae* is widely used due to the combination of the advantages of rapid growth and easy genetic manipulation, as well as possessing an eukaryal post-translational modification machinery, which includes a secretory pathway leading to covalent chemical modifications of proteins and secretion into the extracellular medium (Vieira Gomes et al., 2018). Many strategies have been applied to improve protein production and secretion through eliminating bottlenecks in the secretory processes (Bao et al., 2017; de Ruijter et al., 2016; Huang et al., 2018). Nevertheless, a high-level expression of pharmaceutical and industrial proteins can cause cellular stress and therefore limits large-scale production (Gasser et al., 2008). Identification of new gene targets, especially targets that could improve cellular robustness during constant protein production, is desirable for further optimizing

* Corresponding author. Division of Systems and Synthetic Biology, Department of Biology and Biological Engineering, Chalmers University of Technology, SE-412 96, Gothenburg, Sweden.
** Corresponding author. Division of Systems and Synthetic Biology, Department of Biology and Biological Engineering, Chalmers University of Technology, SE-412 96, Gothenburg, Sweden.
E-mail address: cxin@chalmers.se (X. Chen).

https://doi.org/10.1016/j.ymben.2022.04.005
Received 5 January 2022; Received in revised form 22 April 2022; Accepted 25 April 2022
Available online 1 May 2022
1096-7176/© 2022 The Authors. Published by Elsevier Inc. on behalf of International Metabolic Engineering Society. This is an open access article under the CC BY license (http://creativecommons.org/licenses/by/4.0/).

the *S. cerevisiae* platform as a cell factory.

Production of recombinant proteins at high levels often induces both ER stress and oxidative stress (Martínez et al., 2016). The ER is the primary organelle responsible for importing proteins to the secretory pathway, protein folding, modification and quality control. The ER lumen is an oxidative environment that promotes the biochemical reactions required for protein folding (Tu and Weissman, 2004). Correct protein folding is ensured by the formation of disulfide bonds through the protein disulfide isomerase (Pdi1p) and ER oxidoreductase 1 (Ero1p) pathway, using molecular oxygen as terminal electron acceptor, resulting in the generation of reactive oxygen species (ROS) (Tu et al., 2000). Moreover, the recombinant proteins can have a higher propensity to accumulate inside the ER due to the large number of disulfide bonds to be formed at high-level expression (Tyo et al., 2012). Protein accumulation will further sequester the folding capacity in the ER, resulting in protein misfolding and increased ROS generation. To restore the cellular proteostasis, the unfolded protein response (UPR) is activated to promote protein folding, which can also lead to a rise of ROS (Hetz, 2012). At high concentrations, ROS cause oxidative damage to biomolecules, such as proteins, lipids, and DNA, and in extreme cases, lead to cell apoptosis (Giorgio et al., 2007). Earlier studies have shown that strategies that alleviate the generation of oxidative stress can improve recombinant protein production in *Escherichia coli* (Guerrero Montero et al., 2019), *S. cerevisiae* (Martínez et al., 2015) and Chinese hamster ovary (CHO) cells (Chevallier et al., 2020).

These stress-related phenotypes observed from cells expressing recombinant proteins are very similar to those of the amyloid-β peptides (Aβ) yeast model we established previously (Chen et al., 2017; Chen and Petranovic, 2015). Alzheimer's disease (AD) is the most common form of dementia in elderly population, and characterized by progressive neurodegeneration in specific brain regions. The major pathological hallmark of AD is the accumulation of misfolded Aβ peptides (Murphy and LeVine, 2010). By constitutively expressing Aβ42 peptide, the predominant isoform found in AD patients, we mimicked the chronic cytotoxicity during AD pathogenesis in the yeast model (Chen and Petranovic, 2015). Increased Aβ42 production and aggregation triggered a strong ER stress, mitochondrial dysfunction, and elevated ROS production (Chen et al., 2017; Chen and Petranovic, 2015). In our earlier work, we applied a genome-wide synthetic genetic array (SGA) approach on our Aβ42 expression model to screen for genetic mutants, which could alter the Aβ42 cytotoxicity (Chen et al., 2020). From this screen, we identified the riboflavin kinase gene (*FMN1*) and its metabolic product flavin mononucleotide (FMN) to be able to alleviate cellular Aβ42 cytotoxicity. These results indicate that our humanized Aβ42 yeast model provides a useful platform to identify suppressors to reduce Aβ42 cytotoxicity.

As production of proteins, either recombinant proteins for industrial biotechnology or Aβ42 peptides for modeling of a cytotoxic phenotype, causes a protein misfolding burden, ER stress and oxidative stress. Here, we hypothesized that suppressors of Aβ42 cytotoxicity could potentially be used as metabolic engineering targets to alleviate deleterious effects of protein over expression, and subsequently increase the recombinant protein production. From the SGA screen (Chen et al., 2020), we selected resistant mutants with reduced Aβ42 toxicity and sensitive mutants with increased Aβ42 toxicity to investigate their effects on recombinant protein production. Through combinatorial engineering at these targets, we significantly increased our model test protein α-amylase production yield 18.7-fold (Supplementary Fig. 1). The systems biology approaches (transcriptomics and proteomics) and reverse metabolic engineering allowed us to identify potential regulatory hubs in cellular metabolism and protein synthesis that could be subsequently modified for efficient protein production.

2. Results

2.1. A genome-wide SGA screen identifies modulators of Aβ42 toxicity

In our previous study, we applied the SGA technology with our humanized Aβ42 yeast model to screen for genetic mutants in which the Aβ42 cytotoxic phenotype was altered (Chen et al., 2020). On the arrays, each deletion mutant was mated with an Aβ42 expression strain and a control strain, respectively. By comparing the colony sizes of deletion mutants with Aβ42 expression to the respective control, genetic interactions were obtained and the fitness scores were calculated to represent the cytotoxicity phenotype. Scores >0 represent a decrease in Aβ42 cytotoxicity, i.e., these mutants showed increased resistance to Aβ42 toxicity. Scores <0 represent an increased Aβ42 cytotoxicity and these mutants showed increased sensitivity to Aβ42 toxicity (Fig. 1a).

In order to evaluate whether the identified mutants could alleviate detrimental effects of recombinant protein expression and improve protein production, 46 mutants with resistance to Aβ42 toxicity (score >0.45, p-adj < 0.05) and 20 mutants with sensitivity to Aβ42 toxicity (score < −0.7, p-adj < 0.05) were selected for further investigation (Fig. 1a and Supplementary Table 1). Most proteins encoded by the deleted genes were located within the secretory pathway (Supplementary Fig. 2 and Supplementary Table 2). The Gene set enrichment analysis (GSEA) was performed on these mutated genes via spatial analysis of functional enrichment (SAFE) (Baryshnikova, 2018). For the resistant mutants, the enrichment of gene ontology (GO) terms was mainly represented in group 3 (ribosome biogenesis, 42%), group 13 (transcription and chromatin organization, 13%), and group 2 (glycosylation, protein folding/targeting, cell wall biosynthesis, 11%). For the sensitive mutants, the most enriched GO terms belonged to group 2 (glycosylation, protein folding/targeting, cell wall biosynthesis), group 4 (protein degradation), and group 15 (cell polarity and morphogenesis), which respectively accounted for 56%, 17% and 13% of the population (enrichment p value < 0.05, Supplementary Fig. 3, Supplementary Table 3 and Table 4). These findings are consistent with our previous genome-wide transcriptional study, which showed that Aβ42 expression could trigger a strong ER stress, resulting in activation of unfolded protein response (UPR) to improve ER homeostasis by repressing protein biosynthesis and enhancing protein secretion/degradation (Chen et al., 2017).

2.2. The effect of mutants with altered Aβ42 cytotoxicity on protein production

Based on the SGA screen, 46 resistant mutants, which showed decreased Aβ42 toxicity, and 20 sensitive mutants (where Aβ42 toxicity was increased), were selected to evaluate their effects on protein production using single gene deletions and overexpression, respectively. As a model protein, α-amylase (Liu et al., 2012) was expressed from a high-copy plasmid under control of the strong *TDH3* (*GPD*) promoter, with the α-factor leader in front, which has been proved to increase protein secretion (Hou et al., 2012). The protein production was carried out in an optimized culture medium supplemented with 14 amino acids (Wittrup and Benig, 1994) and α-amylase yields (U/DCW) were determined from supernatant after 96 h cultivation. Interestingly, 26 out of these 46 gene deletions significantly changed α-amylase production, with 20 resulting in increased α-amylase production and 6 leading to decreased α-amylase production compared to the control strain (Fig. 1b). Besides these results, some of the single gene deletions significantly reduced the final biomass to less than half of the control level, indicating their essential functions in transcription regulation (*SNF4* and *SNF6*) and mitochondrial function (*LIP2, MRS2, CAT5* and *IMG2*) (Fig. 1b).

Additionally, the target genes from the 20 sensitive mutants were over-expressed individually from a plasmid using the strong constitutive *TEF1* promoter (Supplementary Fig. 4a), their effects on α-amylase

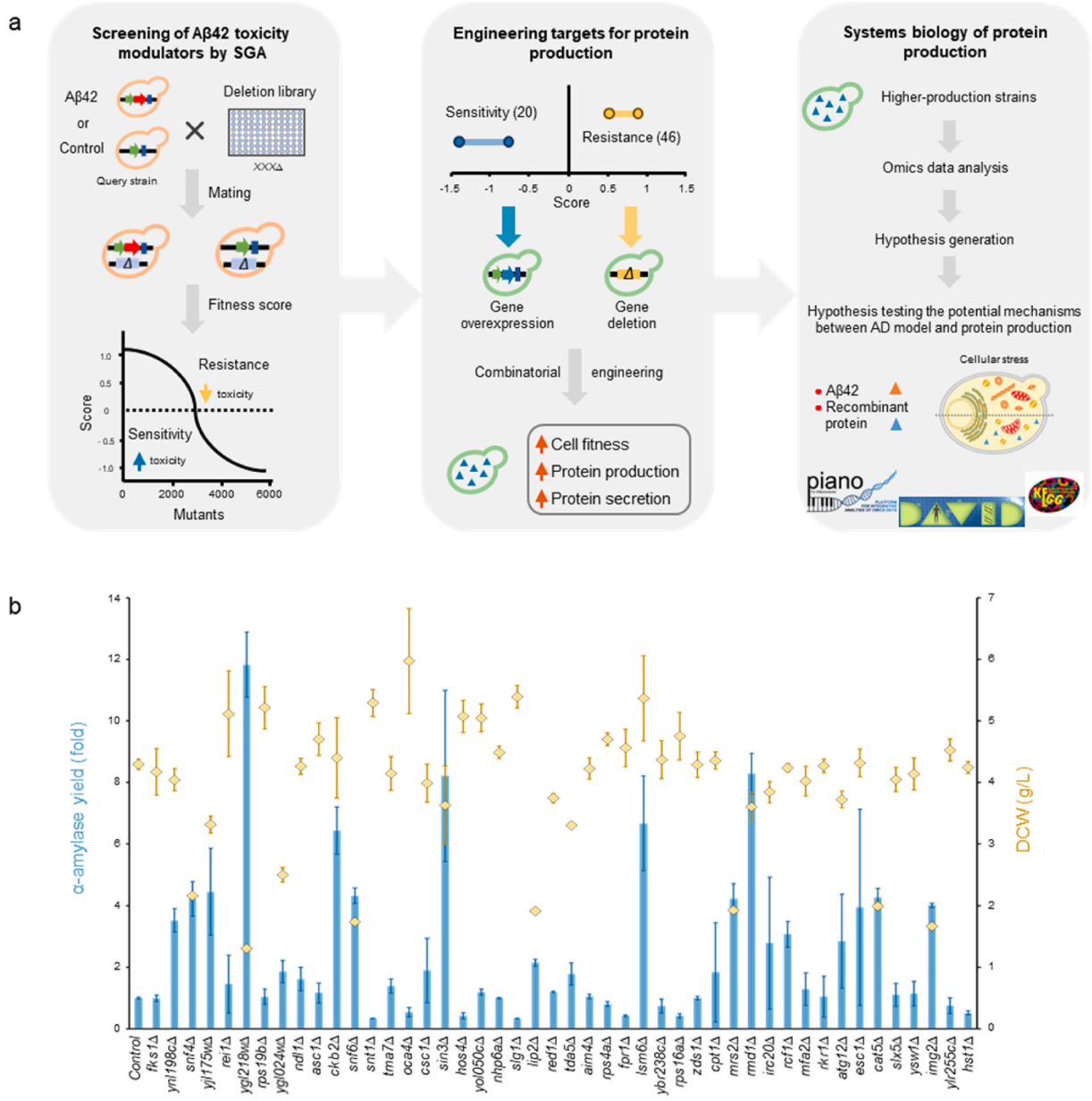

Fig. 1. Roles of suppressors of Aβ42 cytotoxicity in protein production. **a** Schematic workflow for genome-wide synthetic genetic array (SGA) screen of suppressors (Chen et al., 2020) to improve protein production. **b** The effect of 46 single gene deletion strains, which showed decreased Aβ42 toxicity, on α-amylase production (1st round screening). DCW indicates dry cell weight. The α-amylase yield is expressed as U of α-amylase per gram of DCW. The results are shown as the average values ± SD from four independent biological replicates.

production were tested. Out of the 20, only *CDC48* overexpression increased α-amylase production 4.25-fold. On the other hand, 10 out of the 20 single-gene overexpression strains showed significantly decreased α-amylase production, and 9 had no effect (Supplementary Fig. 4b). As 50% of gene overexpression strains presented lower α-amylase production, we suspected that the two-plasmid system with high copy numbers for both α-amylase and target gene overexpression may impose a metabolic burden and cause plasmid instability (Bentley et al., 1990). To solve this problem, we used the AACD strain with the CPOTud system where α-amylase is stably expressed under the *TPI1* promoter in a *tpi1Δ* background strain(Liu et al., 2012) (Supplementary Fig. 5a). Using this strategy, overexpression of four genes (*CDC48*, *GYP1*, *KRE5*, and *ISW1*) led to significantly increased α-amylase production (Supplementary Fig. 5b). These results indicated that the suppressors of Aβ42 toxicity identified from an SGA screen could indeed be applied as potential targets for gene engineering to improve protein production.

2.3. Combinatorial engineering further improves protein production

From the initial screening, the six genes (*YGL218W*, *SIN3*, *RMD1*, *LSM6*, *CKB2,* and *SNF6*) and four genes (*CDC48*, *GYP1*, *KRE5*, and *ISW1*), whose deletion and overexpression, respectively, led to an improved α-amylase production, were chosen for further combinatorial evaluation (Supplementary Fig. 6). As *YGL218W* is an unknown gene with 93% of its open reading frame overlapping with the *MDM34* gene (Supplementary Fig. 7), the deletion of *YGL218W* was replaced by *MDM34* in subsequent experiments. Compared to the control strain A01, the double gene-deletion strains A05 (*lsm6Δsin3Δ*) and A06 (*lsm6Δmdm34Δ*) showed a 9.8-fold and 18.8-fold increase in α-amylase production, respectively, which were higher than the 7.1-fold increase in the single gene-deletion strain A02 (*lsm6Δ*) (Fig. 2a and

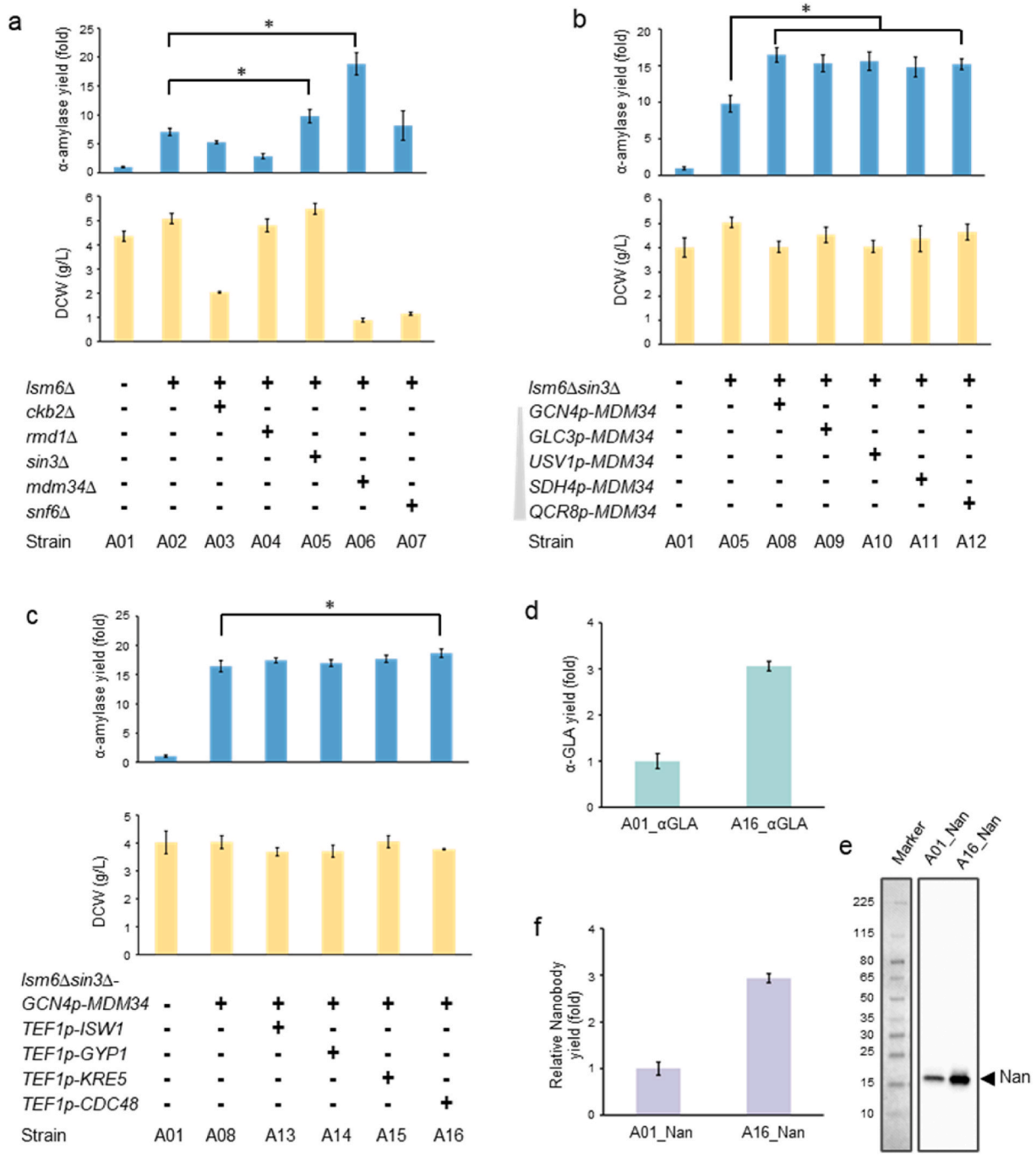

Fig. 2. Combinatorial gene engineering of Aβ42 cytotoxicity suppressors to improve protein production. **a** The effect of double gene-deletion on α-amylase production (2nd round screening). Six candidate genes were selected from the 1st round screening. **b** Fine-tuning of *MDM34* expression via promoter engineering in a *lsm6Δsin3Δ* background (3rd round screening). **c** The effect of overexpression of four candidate genes, whose deletions showed increased Aβ42 toxicity, on α-amylase production in a *lsm6Δsin3ΔGCN4p-MDM34* background (4th round screening). Four genes were selected from the 1st round screening. **d** The expression of *R. oryzae* glucan 1,4-α-glucosidase (α-GLA) in engineered strain A16 and control strain A01. **e** Western blot analysis of human Nanobody (Nan) expression in engineered A16 strain and control strain A01. **f** The expression of Nanobody was quantified and compared between strain A16 and A01. The results are shown as the average values ± SD from four independent biological replicates. Asterisks (*) indicate significant differences (p value < 0.05).

Supplementary Fig. 8a).

Notably, the deletion of *MDM34* significantly reduced the final biomass to 0.89 g/L in the engineered strain, compared to 4.35 g/L in the A01 strain (Fig. 2a). The *MDM34* gene encodes one of the mitochondrial components in the ER-mitochondrial encounter structure (ERMES) complex, which plays an essential role in maintaining normal cellular function, such as phospholipid transport, protein import, as well as mitochondrial dynamics (Kornmann et al., 2009). Deletion of *MDM34* greatly reduces the contacts between ER and mitochondria (Légiot et al., 2019). Hence, we set out to fine-tune the expression of *MDM34* to reduce the side effects of this gene deletion on biomass. A group of weaker promoters, exhibiting differential transcriptional activities in response to glucose and ethanol (Keren et al., 2013), were used to substitute the native *MDM34* promoter in the A05 strain (*lsm6Δsin3Δ*). All five evaluated promoters (*GCN4p*, *GLC3p*, *USV1p*, *SHD4p*, and *QCR8p*) led to significantly increased α-amylase production compared with strain A05,

whereas there was no significant difference between evaluated promoters (Fig. 2b). Additionally, the final biomass in these strains was similar to A01. Among these promoter-substituted strains, the strain carrying the *MDM34* gene with the *GCN4p* promoter showed the highest α-amylase production (strain A08, *lsm6Δsin3ΔGCN4p-MDM34*), 16.5-fold compared with A01 (Fig. 2b).

Furthermore, the four overexpression candidate genes (*CDC48*, *GYP1*, *KRE5*, and *ISW1*) were included in the combinatorial engineering. For the stable expression of heterologous genes, genes were chromosomally integrated into the strain A08 (Supplementary Fig. 8b). Out of four overexpression strains, only the strain with overexpression of the *CDC48* gene (A16, *lsm6Δsin3ΔGCN4p-MDM34-TEF1pCDC48*) showed significantly enhanced α-amylase production compared to strain A08 (p value = 0.45), which represented the highest α-amylase production of 18.7-fold compared with A01. Moreover, the biomass of A16 was not significantly changed compared to A01 (Fig. 2c).

To test whether the selected suppressors of Aβ42 toxicity have a generally positive effect on protein production, we evaluated our best engineered strain A16 for its capacity to produce two other heterologous proteins, glucan-1,4-α-glucosidase from *Rhizopus oryzae* and *Camelidae* Nanobody (Nan, antibody single V-type domain) (Wang et al., 2021). Compared to A01, both proteins showed higher production yields (3.1-fold and 2.9-fold, respectively) in A16 (Fig. 2d, e, 2f, and Supplementary Fig. 9).

2.4. Engineered protein production strains redistribute cellular resources

The physiological properties of the best performing strain from each round of combinatorial modification were characterized in shake-flasks, including strain A02, A05, A08, and A16 (Supplementary Fig. 10). The maximal specific growth rates of engineered strains were from 14% to 26% lower than that of the control A01 strain (Supplementary Table 5 and Supplementary Fig. 11a). Along with the increased α-amylase production, the glucose uptake rates, specific ethanol production rates, and specific glycerol production rates in the engineered strains were significantly decreased (Supplementary Table 5, Supplementary Figs. 11b–11c). The observed physiological characterization of engineered strains suggests a metabolic trade-off between the α-amylase production and the cellular metabolism. Additionally, all engineered strains showed lower specific acetate production rates (from 67% to 73% decrease) and acetate yields (from 39% to 47% decrease) compared to A01. The maximal acetate concentration in the supernatant of A16 was the lowest, with a 62% decrease compared to A01 (Supplementary Tables 5–6 and Supplementary Fig. 11d). As one of the byproducts of yeast glucose fermentation, acetate contributes to the cellular oxidative stress and chronological aging (Orlandi et al., 2013; Semchyshyn et al., 2011). The reduced acetate production in the engineered strains with higher α-amylase production indicates reduced cellular stress, which might directly contribute to increased protein production. Previous study has shown that mild shear stress increases recombinant erythropoietin production compared with higher shear stress (Zhan et al., 2020).

2.5. High protein production strain exhibits increased cell size and reduced ROS formation

Previous studies showed that cells grow larger when forced to express excessive amounts of heterologous proteins, which is negatively correlated with the cell growth rate (Kafri et al., 2016). In our study, the improvement of α-amylase production was also associated with the increased cell size in strain A16 (Supplementary Figs. 12a and 12b). Flow cytometry analysis by forward-scatter with logarithmic amplifiers (FSC-Hlog) displayed two distinct peaks for strains A01 and A16, suggesting that A16 had a larger cell size (Supplementary Fig. 12a). The average of the cell diameter of A16 was 6.8 ± 1.2 μm, significantly longer than 4.7 ± 0.6 μm for strain A01 (p value < 0.0001, Supplementary Fig. 12b). The size of the ER membrane was also increased, with a 2-fold increase in A16 compared to A01 (Supplementary Fig. 12c). The ER is a large membrane-bound compartment spreading throughout the cytoplasm, responsible for maintaining cellular proteostasis (Hetz, 2012). Expansion of the ER size is considered as an integral part of cellular processes to alleviate ER stress (Schuck et al., 2009). The expansion of the ER membrane in A16 may enable a reduced ROS production. To test this, we evaluated the cellular ROS levels. Compared with A01, the overall ROS level was 1.7-fold higher in A16 (Supplementary Fig. 12d). Considering that the A16 strain produced 18.7-fold more of α-amylase compared to A01, the increase in α-amylase production was much higher than the increase in ROS.

2.6. Engineered strains show a global transcriptome and proteome remodeling

The identified suppressors of Aβ42 toxicity were found to be involved in multiple cellular networks (Supplementary Fig. 3 and Supplementary Tables 3–4). By performing combinatorial gene engineering, several different networks could be affected and it might become difficult to understand the mechanisms linking the specific modifications to the improved protein production. To get systems-level insight, we thus analyzed the transcriptomes and proteomes of strains A01, A02, A05, A08, and A16.

Using the transcriptomic data, principal component analysis (PCA) showed that all engineered strains had a gene expression profile distinct from control strain A01, and all strains could be clustered into three groups: group 1 contained strain A01, group 2 contained strain A02, and group 3 contained strains A05, A08, and A16 (Fig. 3a). The differentially expressed genes (DEGs) were identified using strain A01 as control. 2615 DEGs were common in all engineered strains (p-adj < 0.01, Fig. 3b). GSEA of these 2615 DEGs revealed that the gene sets related to ribosome biogenesis/assembly, purine/pyrimidine metabolism, transcription and translation were significantly enriched for upregulated genes in the engineered strains. In contrast, the gene sets involved in central carbohydrate metabolism, glycogen/trehalose metabolism, amino acid metabolism, and cellular response to oxidative stress were significantly enriched for downregulated genes (FDR <0.05, Fig. 3c and Supplementary Fig. 13).

We also quantified the global changes at the proteome level. In total 25,137 peptides were identified and matched to 3886 proteins, with high correlation between biological replicates (Supplementary Fig. 14a). The range of median coefficient of variation (CV) was between 4.1 and 6.7% among all the strains (Fig. 3d). The PCA revealed a clear separation between the engineered strains and the control strain, similar to that of the transcriptomic data (Fig. 3e). 1171 proteins were differentially expressed in all engineered strains (p-adj < 0.05, Fig. 3f). The GSEA of these common proteins showed that the significantly enriched protein sets were consistent with the transcriptomic results (FDR <0.05, Fig. 3g and Supplementary Fig. 14b).

2.7. Engineered strains display global tuning of cellular metabolism

The gene sets related to central carbohydrate metabolism were significantly enriched for downregulated genes and corresponding proteins in both the transcriptome and proteome of the engineered strains (Fig. 3c and g, and Supplementary Fig. 15). 11 out of 15 genes encoding glucose transporters were downregulated, which was consistent with the decreased glucose uptake rate (Supplementary Table 5). We found that genes and corresponding proteins involved in glycolysis were significantly downregulated, which was consistent with the decreased maximal specific growth rates, glucose uptake rate, specific ethanol production rate, specific glycerol production rate, and specific acetate production rate in the engineered strains (Supplementary Table 5). In terms of acetate formation, both the transcription and expression of aldehyde dehydrogenase genes (*ALD2*, *ALD3*, *ALD4*, *ALD5*

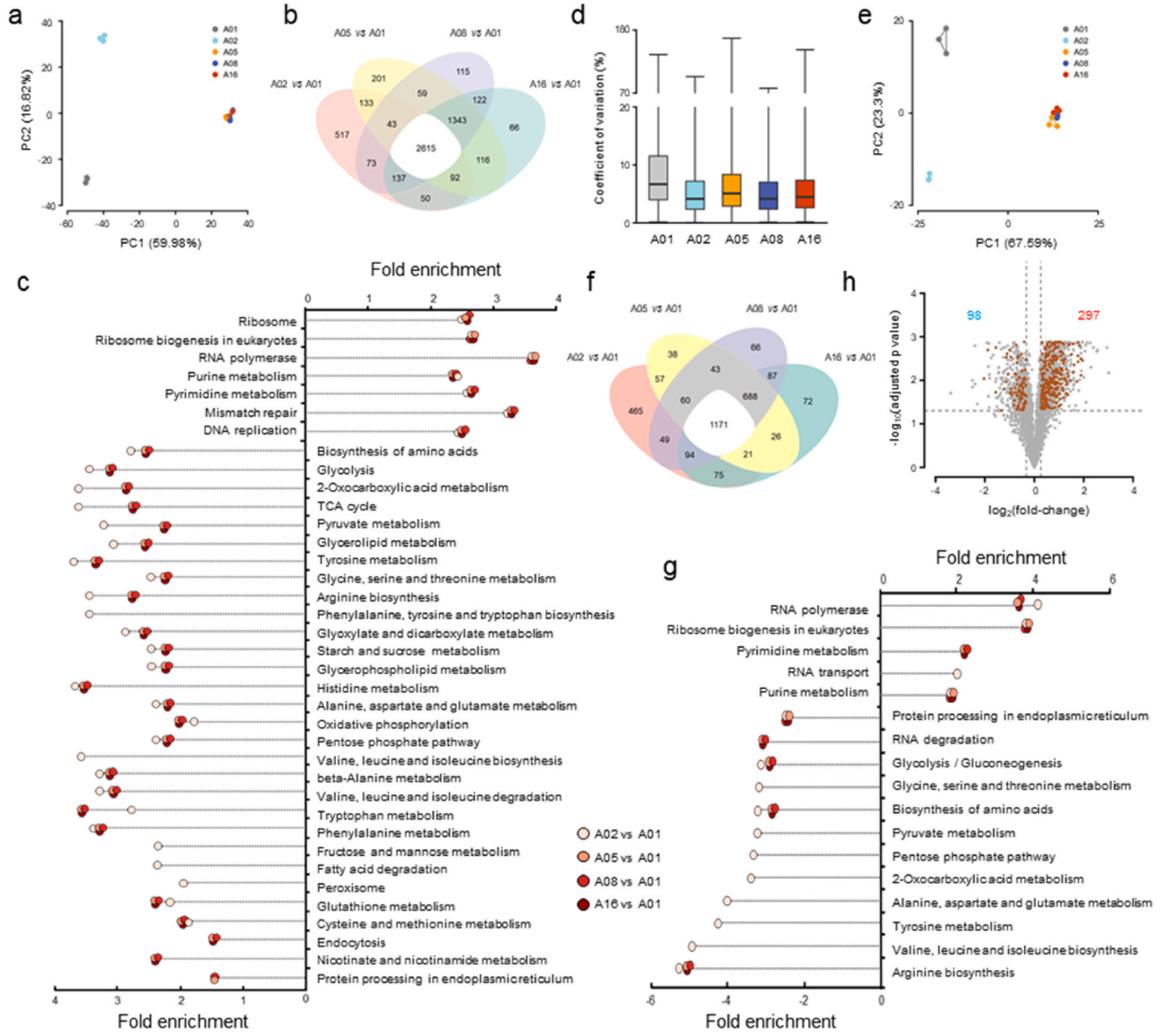

Fig. 3. Transcriptomic and proteomic profiling in engineered strains. **a** PCA of the gene expression in control strain A01 and engineered strains. The gene expression was analyzed in three independent biological replicates. **b** Venn diagram showing distribution of genes differentially expressed between each engineered strain and control strain A01 (p-adj < 0.01), respectively. **c** Gene set enrichment analysis of 2615 genes which are differentially expressed in all engineered strains (FDR <0.05). Fold enrichment indicates the magnitude of enrichment in each comparison. **d** Coefficient of variation of the quantified proteome. The boxes capture lower quartile and upper quartile with median as a horizontal line, whiskers indicate minimum and maximum. **e** PCA of the protein expression in control strain A01 and engineered strains. The protein expression data are derived from three independent biological replicates. **f** Venn diagram showing the distribution of proteins differentially expressed between each engineered strain and control strain A01 (p-adj < 0.05), respectively. **g** Gene set enrichment analysis of 1171 proteins which are differentially expressed in all engineered strains (FDR <0.05) compared with control strain A01. **h** Volcano plot of $\log_2$ Fold change vs adjusted p value of proteins differentially expressed between A16 and A01. The dashed vertical line indicates the threshold of Fold change ($\leq$0.8 or $\geq$ 1.2), while the horizontal line indicates the threshold of statistical significance (p-adj < 0.05). The highlighted points indicate proteins involved in the term information storage and processing, which was represented by 98 and 297 downregulated and upregulated proteins, respectively.

and *ALD6*) related to its production were downregulated, along with a strong upregulation of acetyl-CoA synthetase (ACS1), which is responsible for its catabolism (Supplementary Fig. 15). This finding is consistent with the low acetate yield and reduced maximum acetate concentration in the medium (Supplementary Table 6). The TCA cycle and electron transport chain were significantly upregulated in the engineered strains (Supplementary Fig. 16), which generates 10 times more ATP per glucose than the fermentative pathway (van Dijken et al., 2000). As protein synthesis is an energy consuming process, increased ATP production efficiency could help to meet the enhanced energy demand in higher α-amylase production strains.

The metabolic pathways of two reserve carbohydrates, glycogen and trehalose, were downregulated in the engineered strains (Supplementary Fig. 17). Previous work has shown that depending on growth rate, *S. cerevisiae* can increase its protein content (g/g dry cell weight (DCW)) by decreasing the cellular glycogen and trehalose contents to zero (Nissen et al., 1997). Deletion of *PGM2*, encoding phosphoglucomutase in the glycogen metabolism, results in 30–45% improvement in protein production (Huang et al., 2017). The expression of *PGM2* gene and its corresponding protein (Pgm2p) was significantly decreased in the

engineered strains compared to A01 (p-adj < 0.05).

The genes related to ribosome biosynthesis/assembly, transcription, and translation were mainly upregulated in the engineered strains (Fig. 3c and g and Supplementary Figs. 13 and 14b). This could principally be due to the deletion of *SIN3* and *LSM6*. *SIN3* works as negative regulator of transcription in yeast (Grzenda et al., 2009), while *LSM6* plays roles in RNA processing and degradation (Ingelfinger et al., 2002). Accordingly, a number of transcription and translation related proteins were upregulated in all engineered strains (p-adj < 0.05, Fig. 3h and Supplementary Fig. 18). The purine and pyrimidine metabolic pathways were upregulated as well (Supplementary Figs. 19 and 20). Besides being building blocks of nucleic acids, most purine and pyrimidine nucleotides such as ATP, GTP, UTP, and CTP, also represent sources of energy that drive important cellular reactions (Moffatt and Ashihara, 2002). In addition, in our engineered strains, the proteins involved in biogenesis of iron-sulfur clusters were mostly upregulated (Supplementary Fig. 21). Iron-sulfur clusters play important roles in maintenance of DNA integrity, regulation of gene transcription and protein translation, and energy production(Cardenas-Rodriguez et al., 2018). These findings demonstrate that cells may improve the transcription and translation efficiency from different aspects to meet the increased demand for protein production.

2.8. Reporter TF analysis shows reduced stress response in engineered strains

To explore the underlying transcriptional regulatory response in the engineered strains, we identified the reporter transcription factors (TFs) by integrating the transcriptomics data with the TF network (Oliveira et al., 2008). In total, 67 reporter TFs were scored by the modulation of gene expression controlled by these TFs (p-adj < 0.05, Supplementary Fig. 22a and Supplementary Table 7). The genes regulated by 8 out of 67 reporter TFs were upregulated, all of these 8 TFs were associated with transcriptional regulation. This is consistent with the GSEA results showing that transcription-related processes are upregulated (Fig. 3c and g and Supplementary Figs. 13 and 14b). Among the top downregulation-associated reporter TFs, most were related to stress response, amino acid metabolism, and carbohydrate metabolism. The expression changes of the reporter TFs themselves on the transcriptional level are presented in Supplementary Fig. 22b.

In yeast, Msn2p and Msn4p are crucial transcriptional regulators in response to stress conditions including heat shock, oxidative stress, protein misfolding/unfolding, and osmotic stress (Gasch et al., 2000). The reporter TF analysis showed the downregulation of genes regulated by Msn2p and Msn4p in all engineered strains (Supplementary Fig. 22a). Moreover, the expression of *MSN2* and *MSN4* was also found decreased in all engineered strains and the A16 strain, respectively (Supplementary Fig. 22b). We further validated whether the *MSN2* and *MSN4* played roles in the regulation of protein production. Deletion of either *MSN2* or *MSN4* in the strain A01 improved the α-amylase production 29% and 21%, respectively (p-adj < 0.05, Supplementary Fig. 23a). Yap2p is a transcriptional activator involved in the oxidative stress response. As the reporter TF analysis showed the downregulation of genes regulated by Yap2p in all engineered strains (Supplementary Fig. 22a), *YAP2* was deleted in strain A01, which resulted in a 49% increase of α-amylase production (Supplementary Fig. 23a). Heterologous protein production often contributes to a protein folding burden and causes oxidative stress in the ER (Malhotra et al., 2008). Under these conditions, the UPR is activated to reduce ER stress by triggering the synthesis of transcriptional activator Hac1p, which induces the expression of over 300 target genes (Ron and Walter, 2007). *ERO1* and *PDI1* are target genes of Hac1p, responsible for correct protein folding (Tu et al., 2000). It was noticed that *HAC1*, *ERO1/PDI1* and Ero1p/Pdi1p expression were downregulated in group 3 engineered strains, compared to control strain A01 (Supplementary Figs. 23b and 23c). These results suggested that the transcriptional regulation of oxidative stress response and the UPR are not the major mechanisms to release oxidative stress in the engineered strains with higher α-amylase production.

2.9. Activation of lipid biosynthesis improves protein production

Ergosterol plays crucial roles in membrane biogenesis and function in *S. cerevisiae* (Zhang and Rao, 2010). GSEA pointed to an upregulation of ergosterol biosynthetic processes in group 3 engineered strains (Fig. 4a and Supplementary Fig. 14b). This finding is consistent with the increased cell size and ER membrane size we found in strain A16 (Supplementary Figs. 12a–12c). The production of ergosterol requires sufficient incorporation of heme to Erg11p and Erg5p as a cofactor (Fig. 4a). The availability of heme might be a potential bottleneck in limiting the biosynthesis of ergosterol (Jordá and Puig, 2020). In *S. cerevisiae*, heme is endogenously synthesized in the cytosolic and mitochondrial compartments (Fig. 4b). Studies have shown that overexpression of rate-limiting enzymes in heme biosynthesis can increase the intracellular heme level (Liu et al., 2014; Michener et al., 2012). *HEM3* and *HEM13* encode porphobilinogen deaminase and coproporphyrinogen III oxidase in the heme biosynthetic pathway, respectively. The expression of Hem3p and Hem13p was significantly upregulated in the group 3 engineered strains compared to A01 (Fig. 4b). Rox1p is a transcriptional repressor, which can inhibit the transcription of HEM13 (Keng, 1992). *HMX1*, encoding heme oxygenase, is responsible for the heme degradation (Protchenko and Philpott, 2003). Previous studies illustrated that the inactivation of *ROX1* (Ishchuk et al., 2021; Zhang et al., 2017) or *HMX1* (Ishchuk et al., 2021; Protchenko and Philpott, 2003) expression could elevate the intracellular heme level. In addition, we observed significantly reduced *ROX1* gene expression in group 3 engineered strains (Supplementary Fig. 22b). We further tested whether engineering of heme production would be beneficial for heterologous protein production. Three approaches were implemented to regulate heme metabolism, 1) overexpression of *HEM3* or *HEM13*; 2) deletion of *ROX1* or *HMX1*; 3) combination of *HEM3* or *HEM13* overexpression with *HMX1* deletion. A significantly increased α-amylase production was observed for the *HEM3*-overexpressing and *HEM13*-overexpressing strains, representing a 1.5-fold increase in both strains relative to the control strain. Deletion of *ROX1* and *HMX1* increased α-amylase production 1.4-fold and 1.5-fold, respectively. The production of α-amylase was further increased in the combinatorial strains *TEF1p-HEM3-hmx1Δ* and *TEF1p-HEM13-hmx1Δ*, which showed a 1.8-fold and 1.9-fold increase, respectively (Fig. 4c). As excessive free heme may drive oxidative stress (Quintela-Carvalho et al., 2017), we measured the ROS levels in the combinational strains. ROS levels were not affected in the combinational stains, compared to the control strain (Fig. 4d).

Besides ergosterol, phospholipids are the major components of the yeast cell membrane. The gene sets related to phospholipid metabolism were not enriched for DEGs. However, the reporter TF analysis showed downregulation of genes regulated by Ino2p and Ino4p in all engineered strains (Supplementary Fig. 22a). Ino2p and Ino4p are transcription activators that control the *de novo* synthesis of phospholipids (Schwank et al., 1995) (Fig. 4e). On the other hand, the expression of the *OPI1* gene, encoding a transcriptional repressor for phospholipid synthesis (Fig. 4e), was also downregulated in all engineered strains. Studies in yeast have shown that an *opi1Δ* strain has an expanded ER membrane and alleviated ER stress (Schuck et al., 2009), which boosts the recombinant protein production yield (de Ruijter et al., 2016). Considering the expansion of membrane size in strain A16 (Supplementary Figs. 12a–12c), we speculated that the upregulation of phospholipid synthesis may benefit protein production. To test this experimentally we activated phospholipid synthesis by implementing 1) overexpression of *INO2* or *INO4*; 2) deletion of *OPI1*. A significant increase of α-amylase production was observed in all cases, which was 2.2-fold, 2.0-fold, and 3.0-fold higher in *TEF1p-INO2*, *TEF1p-INO4*, *and opi1Δ*, respectively, compared with the control strain (Fig. 4f). Taken together, one can

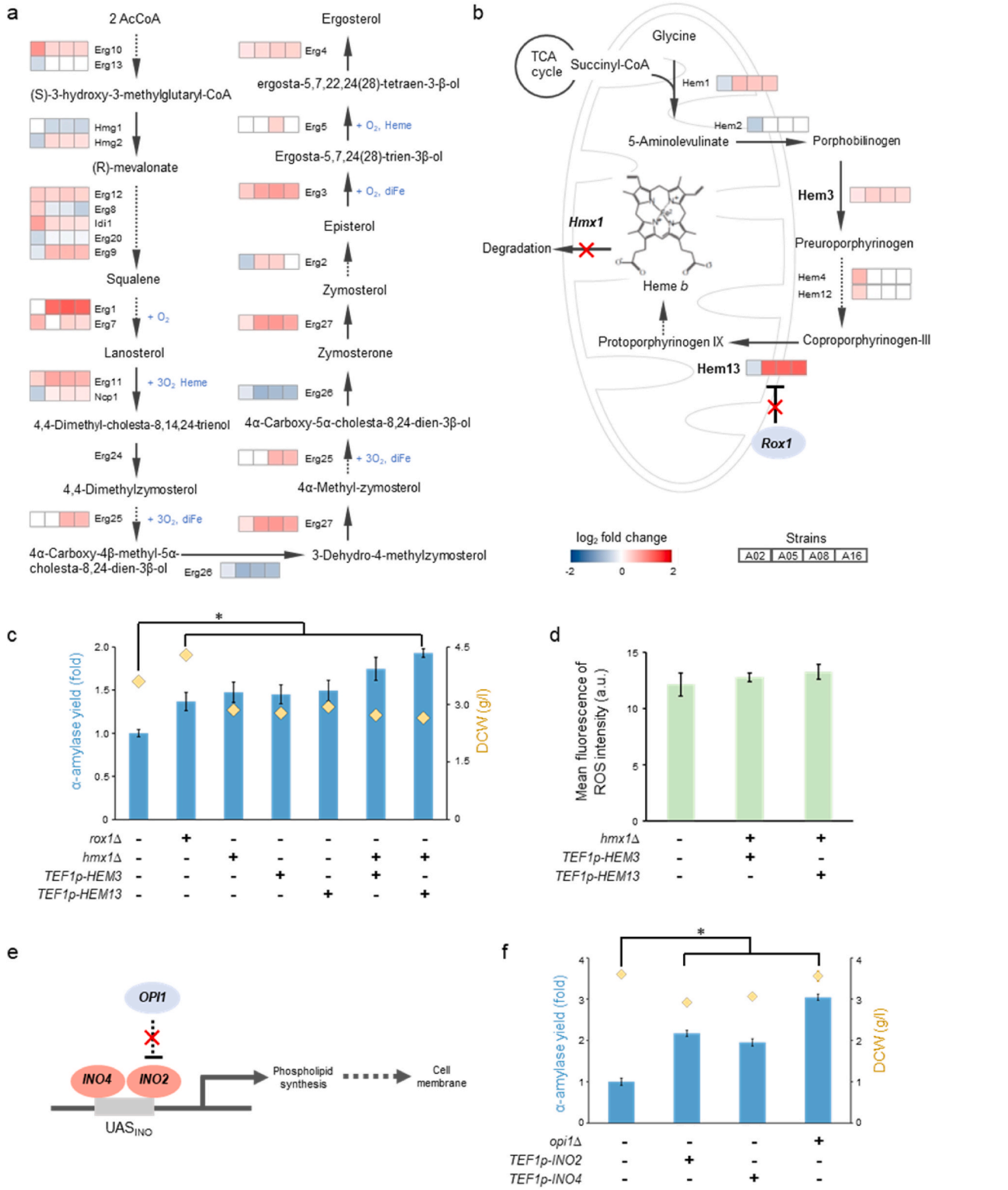

Fig. 4. Activation of lipid biosynthesis improves protein production. **a** Fold changes of expression of proteins related to ergosterol biosynthesis. **b** Fold changes of expression of proteins related to heme biosynthesis. All engineered strains are compared to control strain A01 (p-adj < 0.05). The genetic modifications performed to improve heme production are highlighted in bold. Gene deletions are marked with a red cross. **c** Production of α-amylase upon engineering of the heme metabolism. **d** Flow cytometry analysis of intracellular ROS via dihydrorhodamine 123 (DHR123) staining in heme engineered strains. **e** Schematic illustration of the genetic modifications performed to activate phospholipid biosynthesis. Genes in a blue circle encode transcriptional repressors while those in a red circle represent transcriptional activators. **f** Production of α-amylase upon engineering of phospholipid metabolism. The results are shown as the average values ± SD from four independent biological replicates. Asterisks (*) indicate significant differences (p value < 0.05).

speculate that the activation of lipid biosynthesis can improve protein production by expanding the membrane size. This would assist in a reduction in cellular stress and ER stress, accommodate more intracellular proteins, and provide an increased surface for secretion.

2.10. Repression of arginine biosynthesis improves protein production

Although amino acids are building blocks for protein biosynthesis, genes and corresponding proteins related to amino acid metabolism were downregulated in all engineered strains with higher α-amylase production (Fig. 3c and g, and Supplementary Figs. 13 and 14b). On the other hand, genes encoding amino acid transporters, *SUL1*, *SUL2*, *TAT1*, *DIP5*, *BAP2*, *BAP3*, *GNP1*, and their corresponding proteins were significantly upregulated. Considering that the strains were cultivated in the culture medium with supplementation of 14 amino acids, the enhanced protein production in the engineered strains may be achieved via the increased amino acid uptake. In addition, we observed that most enzymes involved in arginine biosynthesis were significantly downregulated on both transcriptional and protein levels (Fig. 5a and b). Reporter TF analysis showed that genes regulated by Gcn4p, Arg81p, Arg80p were downregulated in all engineered strains (Supplementary Fig. 22a). Gcn4p is a key transcriptional activator for multiple amino acids biosynthesis genes (Mittal et al., 2017). Arg81p and Arg80p are transcriptional factors involved in regulation of arginine-responsive genes (Dubois and Messenguy, 1985).

To experimentally investigate the impact of reduced arginine biosynthesis on protein production, we individually deleted *GCN4*, *ARG81*, and *ARG80*. The α-amylase production was increased 1.8-fold, 1.6-fold, and 1.5-fold in *gcn4Δ*, *arg81Δ*, and *arg80Δ* strains, respectively, compared to A01 (Fig. 5c). Furthermore, we downregulated arginine biosynthesis via applying CRISPR interference (CRISPRi) (Larson et al., 2013) to repress the expression of two genes *ARG3* (Crabeel et al., 1981) and *ARG4* (Beacham et al., 1984). Three single guide RNAs (sgRNAs) were selected for each gene, which targeted the promoter region and repressed the transcription initiation (Supplementary Fig. 24a). For *ARG3*, 2 out of 3 sgRNAs significantly elevated α-amylase production, resulting in a 3.6-fold and 1.7-fold increase compared to the control, respectively (Fig. 5d). Upon *ARG4* downregulation using the 3 sgRNAs, the α-amylase production was increased 1.6-fold, 1.4-fold, and 1.3-fold, respectively (p value < 0.05, Fig. 5d). Nicotinamide adenine dinucleotide phosphate (NADPH) is one of antioxidant molecules to maintain cellular redox homeostasis (Agledal et al., 2010). The downregulated arginine biosynthetic pathway was found along with a reduced NADPH to $NADP^+$ consumption (Fig. 5a), which likely contributes to the intracellular reducing environment. Indeed, the increased α-amylase production did not elevate ROS levels (Fig. 5e).

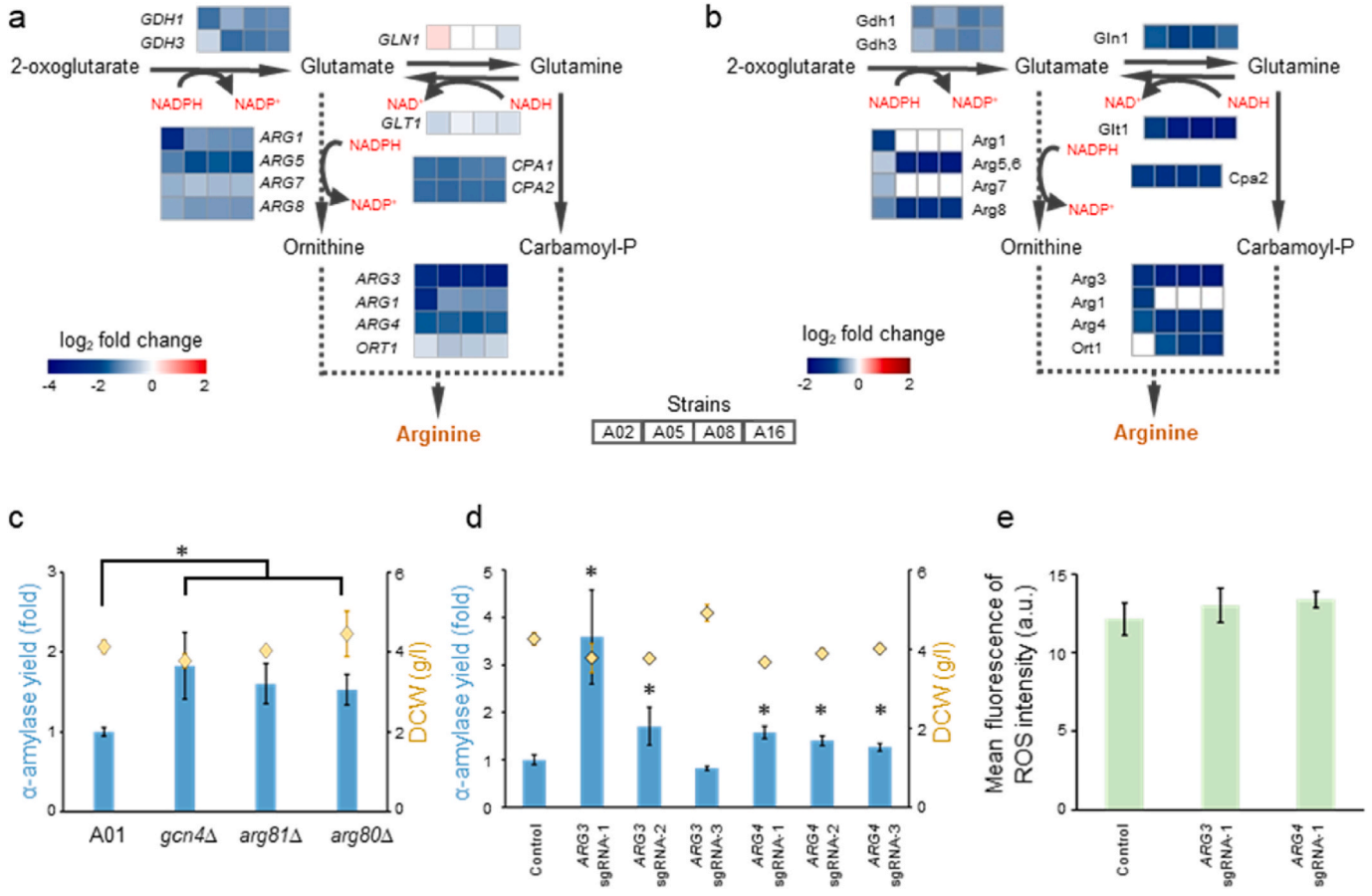

Fig. 5. Repression of arginine biosynthesis improves protein production. **a** Fold changes of gene expression in arginine biosynthesis. **b** Fold changes of protein expression related to arginine biosynthesis. All comparisons are between engineered strains and control strain A01 (p-adj < 0.05). **c** Production of α-amylase upon deletion of transcription factor genes. **d** Production of α-amylase upon repression of *ARG3* and *ARG4* expression via CRISPRi. The *ARG3*-encoded enzyme catalyzes the biosynthesis of arginine precursor citrulline, and the *ARG4*-encoded enzyme catalyzes the final step in the arginine biosynthesis pathway. Three sgRNA were selected for each gene to repress the transcription initiation. Control indicated α-amylase expression in dCas9 background strain. **e** Flow cytometry analysis of intracellular ROS via DHR123 staining in the engineered strains with repressed *ARG3* and *ARG4* expression, respectively. The results are shown as the average values ± SD from three independent biological replicates. Asterisks (*) indicate significant differences (p value < 0.05).

2.11. Repression of sulfur amino acid biosynthesis improves protein production

Reporter TF analysis showed that genes regulated by Met4p and Met32p were downregulated in all engineered strains (Supplementary Fig. 22a). It is known that the transcriptional activator Met4p interacts with Met32p to regulate the sulfur amino acid metabolism (Carrillo et al., 2012). Accordingly, upon the deletion of *MET32*, the α-amylase production was increased 5.0-fold relative to the control strain (p value < 0.05, Supplementary Fig. 25). Methionine and cysteine are the two sulfur-containing proteinogenic amino acids. Most of the genes and corresponding proteins in the methionine and cysteine biosynthetic pathways were found to be downregulated (Fig. 6a and b). As an essential amino acid, 0.7 mM methionine was supplemented in the culture medium. To test whether methionine levels could contribute towards protein production, we evaluated α-amylase production in the presence of different concentrations of methionine in the culture medium. A significantly increased α-amylase production was observed at 0.175 mM and 0.0875 mM methionine added, respectively (Fig. 6c).

Cysteine plays a critical role in protein folding/stability and redox activity by forming disulfide bonds with other cysteine residues (Liu et al., 2016). During cysteine biosynthesis, Cys3p and Cys4p catalyze the two reactions involved in the transsulfuration pathway that converts homocysteine to cysteine (Cherest et al., 1993). The expression of the *CYS4* gene and its corresponding protein was significantly increased in group 3 engineered strains, while *CYS3* gene expression was increased in A02 and A05 compared to the control strain A01 (Fig. 6a and b). As cysteine was not supplied in the culture medium, we first evaluated if increased cysteine levels could improve protein production. Upon addition of different concentrations of cysteine to the culture medium (0.25 mM, 0.5 mM, and 1 mM), no impact on α-amylase production was observed (Fig. 6d). Conversely, we downregulated cysteine biosynthesis via repressing the *CYS3* and *CYS4* gene expression. For each gene, three sgRNAs were selected to repress transcription (Supplementary Fig. 24a).

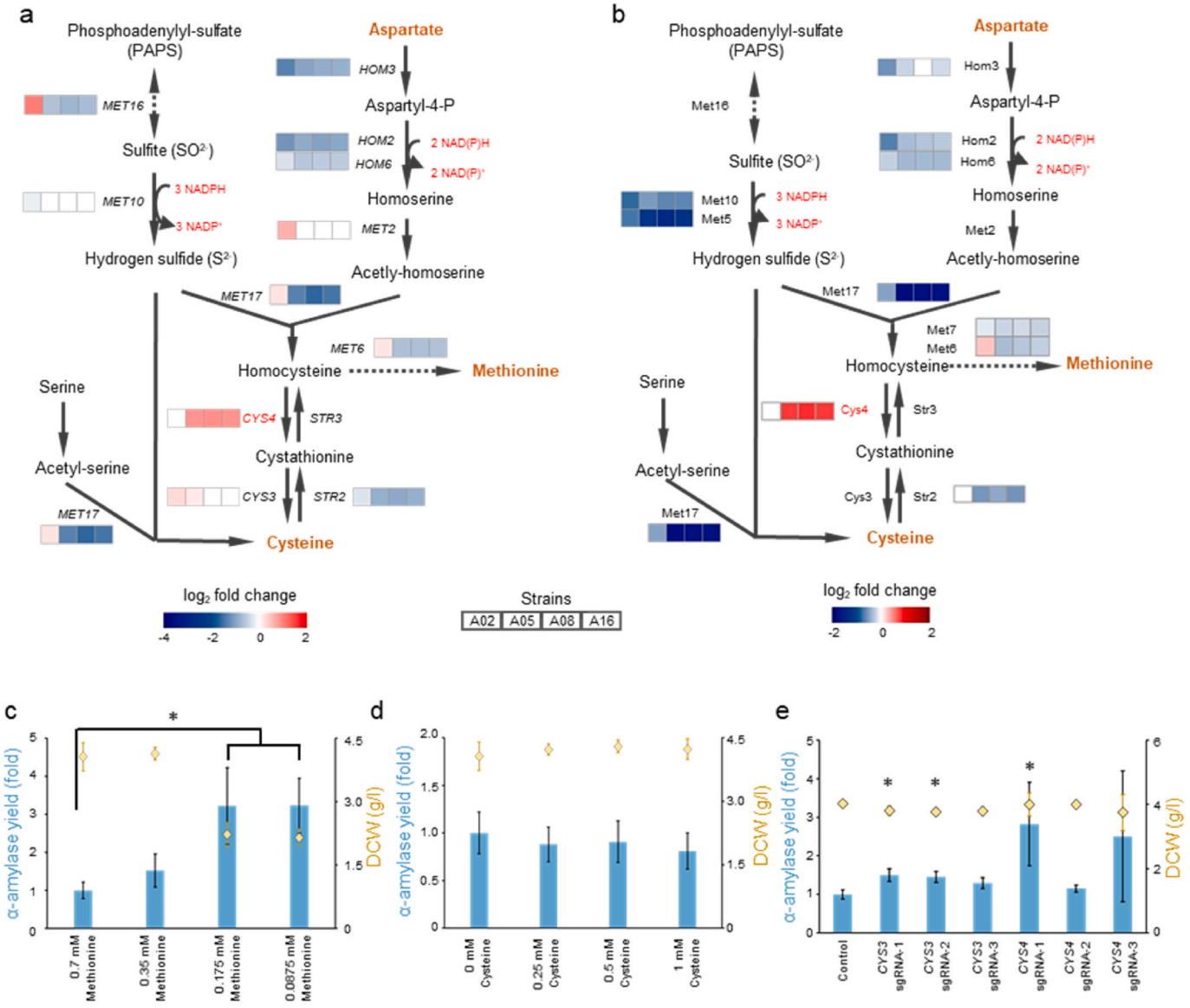

Fig. 6. Repression of sulfur amino acid biosynthesis improves protein production. **a** Fold changes of gene expression related to methionine and cysteine biosynthesis. **b** Fold changes of protein expression related to methionine and cysteine biosynthesis. All comparisons are between engineered strains and control strain A01 (p-adj < 0.05). **c** Production of α-amylase upon reducing the methionine concentrations supplemented in the culture medium. **d** Production of α-amylase with different concentrations of cysteine supplemented in the culture medium. **e** Production of α-amylase upon repression of *CYS3* and *CYS4* expression via CRISPRi. For each gene, three sgRNA were selected repressing the transcription initiation. Control indicated α-amylase expression in dCas9 background strain. The results are shown as the average values ± SD from three independent biological replicates. Asterisks (*) indicate significant differences (p value < 0.05).

For *CYS3*, 2 out of 3 sgRNAs significantly elevated α-amylase production, which was 1.5-fold higher in both strains, compared to control strain (Fig. 6e). For *CYS4*, a 2.8-fold increase in α-amylase production was found for one of the sgRNAs (p value < 0.05, Fig. 6e). Hence, these results indicated that attenuating the sulfur amino acid supply could contribute to improved recombinant protein production.

3. Discussion

In this study, we investigated the roles of suppressors of Aβ42 cytotoxicity on optimizing recombinant protein production. Through an SGA screen (Chen et al., 2020) and metabolic engineering approaches, we identified a subset of genes, which had an effect on protein production. In our engineering strategy, genes that were identified to reduce Aβ42 toxicity were knocked out, while the strong constitutive promoter *TEF1* was used for overexpression of genes that led to increased Aβ42 toxicity upon deletion. Furthermore, combinatorial engineering was applied to combine the genetic modifications, resulting in improved production of our model protein α-amylase. In the best performance strain A16, we had deleted *LSM6* and *SIN3*, downregulated *MDM34* expression, and overexpressed *CDC48*. None of these four targets have been identified to be associated with recombinant protein production in previous studies.

The deletion of *LSM6* and *SIN3* substantially increased recombinant protein production. In yeast, Lsm6p is known to play role in pre-mRNA splicing as a component of the U4/U6–U5 tri-snRNP (small nuclear ribonucleoproteins) (Séraphin, 1995). The cytoplasmic Lsm6p is thought to be involved in mRNA degradation (He and Parker, 2000), while the nuclear Lsm6p is involved in RNA processing (Beggs, 2005). Sin3p is a transcriptional corepressor via associated histone deacetylases (HDACs), required for general repression of transcription. As a result, the Sin3p/HDAC complex is involved in vital biological processes, including cell proliferation, energy metabolism, and cellular senescence (Chaubal and Pile, 2018; Grzenda et al., 2009). Transcriptomic studies from yeast (Bernstein et al., 2000), *Drosophila* (Chaubal and Pile, 2018), and mouse (Dannenberg et al., 2005) demonstrated the important role of the Sin3 complex in the regulation of gene transcription. In our transcriptomic and proteomic data, the group 3 strains A05, A08, and A16 shared a large number of regulation patterns distinct from control strain A01 and strain A02, indicating the contribution of *sin3Δ*. Transcription and translation are crucial checkpoints for protein production as they determine the production efficiency from DNA to peptide (Rodnina, 2016). The deletion of *LSM6* and *SIN3* could release the repression on transcription and translation, which may explain our findings that the gene sets related to RNA processing, transcription, and translation were upregulated in the deletion strains. It suggested that *LSM6* and *SIN3* are promising gene targets for further exploration in the design of efficient cell factories.

CDC48 encodes an essential and highly conserved AAA + ATPase (ATPase associated with diverse cellular activities) with protein-unfoldase activity. A recent *in vitro* study indicated that Cdc48p can generate unfolded segments in ubiquitinated proteins for subsequent engagement and degradation by the 26S proteasome (Olszewski et al., 2019). In a humanized Huntington's disease (HD) yeast model, the Cdc48 segregase machinery can promote the disaggregation of ubiquitinated HTT103QP protein aggregates, which facilitates ubiquitin recycling and misfolded protein degradation (Higgins et al., 2020). Stress granules (SGs) are aggregates composed of untranslated messenger ribonucleoproteins (mRNPs) that usually form upon cellular stress. Mutations that cause persistent or aberrant SGs formation often contribute to pathogenesis of neurodegenerative diseases (NDs) (Wolozin and Ivanov, 2019). A genetic screen in *S. cerevisiae* showed that Cdc48p can target SGs to the vacuole for autophagic clearance (Buchan et al., 2013). We also observed increased Aβ42 cytotoxicity in the *cdc48Δ* strain from the SGA screen, suggesting that Cdc48p might be a contributing factor towards Aβ42 detoxification via clearing misfolded proteins and toxic RNPs. The overexpression of *CDC48* also increased the α-amylase production, which may be due to the alleviation of misfolded protein stress and increased protein turnover. Further investigation on the biological significance of Cdc48p could improve our understanding as well as help determine its potential as a metabolic engineering target.

Although Lsm6p, Sin3p, Mdm34p, and Cdc48p play diverse functions in vital biological processes that could directly or indirectly influence protein formation, our transcriptomics and proteomics analyses showed that the combination of these suppressors also imposed a global regulation on cellular metabolism that might be beneficial for protein production (Fig. 7). In the engineered strains, we observed that the glycolysis pathway was downregulated. Previous studies showed that the glycolysis pathway is enriched with functionally redundant paralogs, and 12 glycolytic enzymes which convert glucose to ethanol are encoded by 27 paralogs (Solis-Escalante et al., 2015). By downregulating glycolytic genes, yeast cells may allocate more of their proteome to recombinant protein production. Studies demonstrated the positive correlation between anerobic glycolysis and cell proliferation (Lunt and Heiden, 2011; Vander Heiden et al., 2009). The downregulated glycolysis was coupled with reduced maximum specific growth rates and glucose uptake rates in the engineered strains. As a byproduct of ethanol fermentation, the accumulated acetate is detrimental to recombinant protein production (De Mey et al., 2007). The significantly reduced acetate production rates and acetate yields in our engineered strains may therefore be beneficial for stress resistance and protein production.

Increased protein production and secretion requires membrane and transport vesicles in the secretory pathway, which are mainly dependent on lipid biosynthesis. A study in *S. pombe* showed that lipid biosynthesis can limit protein secretion (Klein et al., 2014). Recent studies showed that engineering the vesicle machinery could increase the secretion of recombinant proteins in both *S. cerevisiae* (Hou et al., 2012) and mammalian cells (Peng et al., 2010). In our engineered strains we observed significantly upregulated expression of genes related to the ergosterol biosynthesis pathway. Reverse metabolic engineering strategy that targeted the production of heme (cofactor in ergosterol biosynthesis pathway) and phospholipid biosynthesis could improve α-amylase production. The increased lipid biosynthesis may help release ER stress and facilitate the secretion of α-amylase. In support of this hypothesis, we also observed a reduced ROS formation in the heme-pathway engineered strains. Targeting lipid metabolism and cofactors may be a reasonable strategy for metabolic engineering of protein production.

Amino acids are building blocks for protein synthesis. In this study, both transcriptome and proteome analyses showed that amino acid biosynthesis pathways were downregulated in the engineered strains whereas the genes encoding amino acid transporters and their corresponding proteins were significantly upregulated. Considering that the culture medium is supplemented with 14 amino acids, these results indicated that the engineered strains shift from amino acid biosynthesis to increased amino acid uptake. A recent study in *S. cerevisiae* showed that cells cultivated in rich medium with amino acid supply exhibit a higher uptake of arginine, methionine, and threonine than their biosynthesis need (Björkeroth et al., 2020). Arginine could serve as a nitrogen source, and cytosolic arginine regulates the expression of arginine synthesis enzymes by repressing them (Ljungdahl and Daignan-Fornier, 2012). The excess uptake of methionine is also associated with lower expression of related biosynthetic enzymes, which results in reduction of the proteome burden by ~4% in rich medium under aerobic condition (Björkeroth et al., 2020). This may explain the significantly downregulated arginine and methionine biosynthetic pathways in our engineered strains. As the total amount of proteins inside a cell is constrained, the orchestration of proteome allocation is crucial for maintaining normal cellular function and proliferation (Nilsson and Nielsen, 2016; Sánchez et al., 2017). The proteome is mainly reallocated from cellular amino acid biosynthesis to cytoplasmic

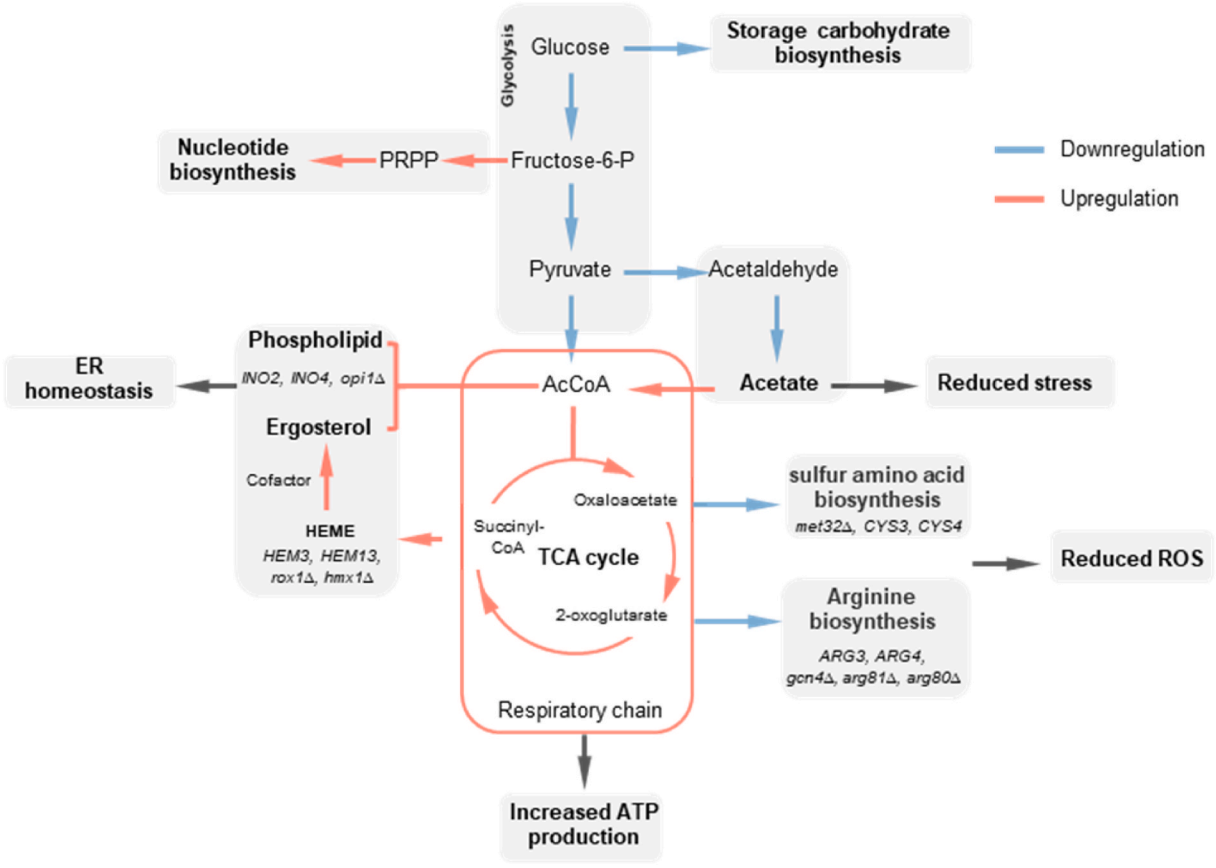

Fig. 7. Proposed model depicting global metabolic tuning to improve protein production. ER stress and oxidative stress derived from the overexpression of recombinant proteins are alleviated via reduced acetate concentration, upregulated membrane lipids biosynthesis, and repression of sulfur amino acid and arginine biosynthesis. Additionally, the suppressors of Aβ42 cytotoxicity can also cause the proteome reallocation to improve recombinant protein production through downregulation of the glycolytic pathway, storage carbohydrate biosynthesis (glycogen and trehalose), and amino acid biosynthesis. Activation of TCA cycle and respiratory chain can provide energetic support by increasing the generation of ATP and NADH. Upregulation of nucleotide biosynthesis (purine and pyrimidine) helps protein production by providing nucleic acids and energy source.

translation in rich medium, which enables an increase in cell growth (Björkeroth et al., 2020). In this study, we observed a proteome allocation to transcription and translation related processes in the engineered strains. This did however not result in increased cell growth, which could be due to the reduced glucose uptake rates and downregulated glycolysis. This might contribute to the increased production of recombinant protein. Similarly, by the downregulation of the biosynthesis of arginine and sulfur amino acids, we observed improved α-amylase production, suggesting that the optimization of proteome allocation could be an interesting approach to metabolic engineering of efficient protein cell factories.

In summary, we investigated novel targets for improved recombinant proteins production in *S. cerevisiae* identified by an SGA screen of suppressors against Aβ42 cytotoxicity. Furthermore, the combinatorial engineering of candidate gene targets followed by detailed omics analysis provided highly informative data regarding the beneficial effects on cellular metabolic activity, oxidative stress alleviation, and proteostasis for improved protein production. Due to the strong conservation of many essential cellular processes among eukaryal cells, our findings can be used as guidelines to design cell factories for the production of industrial or pharmaceutical proteins in yeast and possibly other eukaryal hosts.

4. Methods

Methods are provided in *SI Appendix, Methods*. These include plasmids and strains, media and growth conditions, SGA analysis, fermentation, biomass and extracellular analyses, protein quantification, Western blot, ROS measurement, cell size assay, ER staining, transcriptome analysis, sample preparation for proteomic analysis, quantitative proteome analysis, and statistical analysis.

Data availability

The RNA-seq raw data can be downloaded from the Genome Expression Omnibus website (GEO, https://www.ncbi.nlm.nih.gov/geo/) with series number GSE185570. The mass spectrometry proteomics data have been deposited to the ProteomeXchange Consortium via the PRIDE (Perez-Riverol et al., 2019) partner repository with the dataset identifier PXD030111. All study data are included in the article and *SI Appendix*. The materials that were reported in this study are available from the corresponding authors upon reasonable request.

Author statement

Xin Chen: Conceptualization, Formal analysis, Investigation, Methodology, Resources, Validation, Visualization, Writing - original draft and review & editing. **Xiaowei Li:** Investigation, Formal analysis, Writing - review & editing. **Boyang Ji:** Software, Writing - review & editing. **Yanyan Wang:** Methodology, Validation. **Olena P. Ishchuk:** Investigation, Writing - review & editing. **Egor Vorontsov:** Methodology, Writing - review & editing. **Dina Petranovic:** Funding acquisition, Project administration, Writing - review & editing. **Verena Siewers:** Project administration, Supervision, Writing - review & editing. **Martin**

K. M. Engqvist: Project administration, Supervision, Writing - review & editing.

Declaration of competing interests

The authors declare that there are no competing interests.

Acknowledgements

We acknowledge support from the National Genomics Infrastructure in Stockholm funded by Science for Life Laboratory, the Knut and Alice Wallenberg Foundation and the Swedish Research Council, and SNIC/Uppsala Multidisciplinary Center for Advanced Computational Science for assistance with massively parallel sequencing and access to the UPPMAX computational infrastructure. We acknowledge the Proteomics Core Facility at the University of Gothenburg, Sweden. The work was financially supported by the VINNOVA center CellNova (2017-02105) and Novo Nordisk Foundation (NNF10CC1016517).

Appendix A. Supplementary data

Supplementary data to this article can be found online at https://doi.org/10.1016/j.ymben.2022.04.005.

References

Agledal, L., Niere, M., Ziegler, M., 2010. The phosphate makes a difference: cellular functions of NADP. Redox Rep. 15, 2–10.
Bao, J., Huang, M., Petranovic, D., Nielsen, J., Vieille, C., 2017. Moderate expression of SEC16 increases protein secretion by *Saccharomyces cerevisiae*. Appl. Environ. Microbiol. 83, e03400–e03416.
Baryshnikova, A., 2018. Spatial analysis of functional enrichment (SAFE) in large biological networks. Methods Mol. Biol. 1819, 249–268.
Beacham, I.R., Schweitzer, B.W., Warrick, H.M., Carbon, J., 1984. The nucleotide sequence of the yeast *ARG4* gene. Gene 29, 271–279.
Beggs, J.D., 2005. Lsm proteins and RNA processing. Biochem. Soc. Trans. 33, 433–438.
Bentley, W.E., Mirjalili, N., Andersen, D.C., Davis, R.H., Kompala, D.S., 1990. Plasmid-encoded protein: the principal factor in the "metabolic burden" associated with recombinant bacteria. Biotechnol. Bioeng. 35, 668–681.
Bernstein, B.E., Tong, J.K., Schreiber, S.L., 2000. Genomewide studies of histone deacetylase function in yeast. Proc. Natl. Acad. Sci. 97, 13708–13713.
Björkeroth, J., Campbell, K., Malina, C., Yu, R., Di Bartolomeo, F., Nielsen, J., 2020. Proteome reallocation from amino acid biosynthesis to ribosomes enables yeast to grow faster in rich media. Proc. Natl. Acad. Sci. 117, 21804–21812.
Buchan, J.R., Kolaitis, R.M., Taylor, J.P., Parker, R., 2013. Eukaryotic stress granules are cleared by autophagy and Cdc48/VCP function. Cell 153, 1461–1474.
Cardenas-Rodriguez, M., Chatzi, A., Tokatlidis, K., 2018. Iron-sulfur clusters: from metals through mitochondria biogenesis to disease. JBIC 23, 509–520.
Carrillo, E., Ben-Ari, G., Wildenhain, J., Tyers, M., Grammentz, D., Lee, T.A., 2012. Characterizing the roles of *Met31* and *Met32* in coordinating *Met4*-activated transcription in the absence of *Met30*. Mol. Biol. Cell 23, 1928–1942.
Chaubal, A., Pile, L.A., 2018. Same agent, different messages: insight into transcriptional regulation by *SIN3* isoforms. Epigenet. Chromatin 11, 17.
Chen, X., Bisschops, M.M.M., Agarwal, N.R., Ji, B., Shanmugavel, K.P., Petranovic, D., 2017. Interplay of energetics and ER stress exacerbates Alzheimer's amyloid-β (Aβ) toxicity in yeast. Front. Mol. Neurosci. 10, 232.
Chen, X., Ji, B., Hao, X., Li, X., Eisele, F., Nyström, T., Petranovic, D., 2020. FMN reduces Amyloid-β toxicity in yeast by regulating redox status and cellular metabolism. Nat. Commun. 11, 867.
Chen, X., Petranovic, D., 2015. Amyloid-β peptide-induced cytotoxicity and mitochondrial dysfunction in yeast. FEMS Yeast Res. 15.
Cherest, H., Thomas, D., Surdin-Kerjan, Y., 1993. Cysteine biosynthesis in *Saccharomyces cerevisiae* occurs through the transsulfuration pathway which has been built up by enzyme recruitment. J. Bacteriol. 175, 5366–5374.
Chevallier, V., Andersen, M.R., Malphettes, L., 2020. Oxidative stress-alleviating strategies to improve recombinant protein production in CHO cells. Biotechnol. Bioeng. 117, 1172–1186.
Crabeel, M., Messenguy, F., Lacroute, F., Glansdorff, N., 1981. Cloning *arg3*, the gene for ornithine carbamoyltransferase from *Saccharomyces cerevisiae*: expression in *Escherichia coli* requires secondary mutations; production of plasmid beta-lactamase in yeast. Proc. Natl. Acad. Sci. 78, 5026–5030.
Dannenberg, J.-H., David, G., Zhong, S., van der Torre, J., Wong, W.H., Depinho, R.A., 2005. mSin3A corepressor regulates diverse transcriptional networks governing normal and neoplastic growth and survival. Genes Dev. 19, 1581–1595.
De Mey, M., De Maeseneire, S., Soetaert, W., Vandamme, E., 2007. Minimizing acetate formation in E. coli fermentations. J. Ind. Microbiol. 34, 689–700.
de Ruijter, J.C., Koskela, E.V., Frey, A.D., 2016. Enhancing antibody folding and secretion by tailoring the *Saccharomyces cerevisiae* endoplasmic reticulum. Microb. Cell Factories 15, 87.
Dubois, E., Messenguy, F., 1985. Isolation and characterization of the yeast *ARGRII* gene involved in regulating both anabolism and catabolism of arginine. Mol. Gen. Genet. 198, 283–289.
Gasch, A.P., Spellman, P.T., Kao, C.M., Carmel-Harel, O., Eisen, M.B., Storz, G., Botstein, D., Brown, P.O., 2000. Genomic expression programs in the response of yeast cells to environmental changes. Mol. Biol. Cell 11, 4241–4257.
Gasser, B., Saloheimo, M., Rinas, U., Dragosits, M., Rodríguez-Carmona, E., Baumann, K., Giuliani, M., Parrilli, E., Branduardi, P., Lang, C., Porro, D., Ferrer, P., Tutino, M.L., Mattanovich, D., Villaverde, A., 2008. Protein folding and conformational stress in microbial cells producing recombinant proteins: a host comparative overview. Microb. Cell Factories 7, 11, 11.
Giorgio, M., Trinei, M., Migliaccio, E., Pelicci, P.G., 2007. Hydrogen peroxide: a metabolic by-product or a common mediator of ageing signals? Nat. Rev. Mol. Cell Biol. 8, 722–728.
Grzenda, A., Lomberk, G., Zhang, J.-S., Urrutia, R., 2009. Sin3: master scaffold and transcriptional corepressor. BBA 1789, 443–450.
Guerrero Montero, I., Dolata, K.M., Schlüter, R., Malherbe, G., Sievers, S., Zühlke, D., Sura, T., Dave, E., Riedel, K., Robinson, C., 2019. Comparative proteome analysis in an *Escherichia coli* CyDisCo strain identifies stress responses related to protein production, oxidative stress and accumulation of misfolded protein. Microb. Cell Factories 18, 19.
He, W., Parker, R., 2000. Functions of Lsm proteins in mRNA degradation and splicing. Curr. Opin. Cell Biol. 12, 346–350.
Hetz, C., 2012. The unfolded protein response: controlling cell fate decisions under ER stress and beyond. Nat. Rev. Mol. Cell Biol. 13, 89–102.
Higgins, R., Kabbaj, M.-H., Sherwin, D., Howell, L.A., Hatcher, A., Tomko Jr., R.J., Wang, Y., 2020. The Cdc48 complex alleviates the cytotoxicity of misfolded proteins by regulating ubiquitin homeostasis. Cell Rep. 32, 107898, 107898.
Hou, J., Tyo, K., Liu, Z., Petranovic, D., Nielsen, J., 2012. Engineering of vesicle trafficking improves heterologous protein secretion in *Saccharomyces cerevisiae*. Metab. Eng. 14, 120–127.
Huang, M., Bao, J., Hallström, B.M., Petranovic, D., Nielsen, J., 2017. Efficient protein production by yeast requires global tuning of metabolism. Nat. Commun. 8, 1131.
Huang, M., Wang, G., Qin, J., Petranovic, D., Nielsen, J., 2018. Engineering the protein secretory pathway of *Saccharomyces cerevisiae* enables improved protein production. Proc. Natl. Acad. Sci. 115, E11025–E11032.
Ingelfinger, D., Arndt-Jovin, D.J., Lührmann, R., Achsel, T., 2002. The human LSm1-7 proteins colocalize with the mRNA-degrading enzymes Dcp1/2 and Xrnl in distinct cytoplasmic foci. RNA 8, 1489–1501.
Ishchuk, O.P., Frost, A.T., Muñiz-Paredes, F., Matsumoto, S., Laforge, N., Eriksson, N.L., Martínez, J.L., Petranovic, D., 2021. Improved production of human hemoglobin in yeast by engineering hemoglobin degradation. Metab. Eng. 66, 259–267.
Johnson, I.S., 1982. Authenticity and purity of human insulin (recombinant DNA). Diabetes Care 5 (Suppl. 2), 4–12.
Jordá, T., Puig, S., 2020. Regulation of ergosterol biosynthesis in Saccharomyces cerevisiae. Genes 11, 795.
Kafri, M., Metzl-Raz, E., Jona, G., Barkai, N., 2016. The cost of protein production. Cell Rep. 14, 22–31.
Keng, T., 1992. *HAP1* and *ROX1* form a regulatory pathway in the repression of *HEM13* transcription in *Saccharomyces cerevisiae*. Mol. Cell Biol. 12, 2616–2623.
Keren, L., Zackay, O., Lotan-Pompan, M., Barenholz, U., Dekel, E., Sasson, V., Aidelberg, G., Bren, A., Zeevi, D., Weinberger, A., Alon, U., Milo, R., Segal, E., 2013. Promoters maintain their relative activity levels under different growth conditions. Mol. Syst. Biol. 9, 701, 701.
Klein, T., Lange, S., Wilhelm, N., Bureik, M., Yang, T.-H., Heinzle, E., Schneider, K., 2014. Overcoming the metabolic burden of protein secretion in *Schizosaccharomyces pombe* – a quantitative approach using 13C-based metabolic flux analysis. Metab. Eng. 21, 34–45.
Kornmann, B., Currie, E., Collins, S.R., Schuldiner, M., Nunnari, J., Weissman, J.S., Walter, P., 2009. An ER-mitochondria tethering complex revealed by a synthetic biology screen. Science 325, 477–481.
Larson, M.H., Gilbert, L.A., Wang, X., Lim, W.A., Weissman, J.S., Qi, L.S., 2013. CRISPR interference (CRISPRi) for sequence-specific control of gene expression. Nat. Protoc. 8, 2180–2196.
Légiot, A., Céré, C., Dupoiron, T., Kaabouni, M., Camougrand, N., Manon, S., 2019. Mitochondria-Associated Membranes (MAMs) are involved in Bax mitochondrial localization and cytochrome c release. Microb cell (Graz, Austria) 6, 257–266.
Liu, L., Martínez, J.L., Liu, Z., Petranovic, D., Nielsen, J., 2014. Balanced globin protein expression and heme biosynthesis improve production of human hemoglobin in *Saccharomyces cerevisiae*. Metab. Eng. 21, 9–16.
Liu, T., Wang, Y., Luo, X., Li, J., Reed, S.A., Xiao, H., Young, T.S., Schultz, P.G., 2016. Enhancing protein stability with extended disulfide bonds. Proc. Natl. Acad. Sci. 113, 5910–5915.
Liu, Z., Tyo, K.E., Martinez, J.L., Petranovic, D., Nielsen, J., 2012. Different expression systems for production of recombinant proteins in *Saccharomyces cerevisiae*. Biotechnol. Bioeng. 109, 1259–1268.
Ljungdahl, P.O., Daignan-Fornier, B., 2012. Regulation of amino acid, nucleotide, and phosphate metabolism in *Saccharomyces cerevisiae*. Genetics 190, 885–929.
Lunt, S.Y., Heiden, M.G.V., 2011. Aerobic glycolysis: meeting the metabolic requirements of cell proliferation. Annu. Rev. Cell Dev. Biol. 27, 441–464.
Malhotra, J.D., Miao, H., Zhang, K., Wolfson, A., Pennathur, S., Pipe, S.W., Kaufman, R. J., 2008. Antioxidants reduce endoplasmic reticulum stress and improve protein secretion. Proc. Natl. Acad. Sci. 105, 18525–18530.

Martínez, J.L., Liu, L., Petranovic, D., Nielsen, J., 2015. Engineering the oxygen sensing regulation results in an enhanced recombinant human hemoglobin production by *Saccharomyces cerevisiae*. Biotechnol. Bioeng. 112, 181–188.
Martínez, J.L., Meza, E., Petranovic, D., Nielsen, J., 2016. The impact of respiration and oxidative stress response on recombinant α-amylase production by *Saccharomyces cerevisiae*. Metab. Eng. Commun. 3, 205–210.
Michener, J.K., Nielsen, J., Smolke, C.D., 2012. Identification and treatment of heme depletion attributed to overexpression of a lineage of evolved P450 monooxygenases. Proc. Natl. Acad. Sci. 109, 19504–19509.
Mittal, N., Guimaraes, J.C., Gross, T., Schmidt, A., Vina-Vilaseca, A., Nedialkova, D.D., Aeschimann, F., Leidel, S.A., Spang, A., Zavolan, M., 2017. The Gcn4 transcription factor reduces protein synthesis capacity and extends yeast lifespan. Nat. Commun. 8, 457.
Moffatt, B.A., Ashihara, H., 2002. Purine and pyrimidine nucleotide synthesis and metabolism. Arabidopsis Book 1, e0018 e0018.
Murphy, M.P., LeVine 3rd, H., 2010. Alzheimer's disease and the amyloid-beta peptide. J. Alzheim. Dis. 19, 311–323.
Nilsson, A., Nielsen, J., 2016. Metabolic trade-offs in yeast are caused by F1F0-ATP synthase. Sci. Rep. 6, 22264.
Nissen, T.L., Schulze, U., Nielsen, J., Villadsen, J., 1997. Flux distributions in anaerobic, glucose-limited continuous cultures of *Saccharomyces cerevisiae*. Microbiology 143, 203–218.
Oliveira, A.P., Patil, K.R., Nielsen, J., 2008. Architecture of transcriptional regulatory circuits is knitted over the topology of bio-molecular interaction networks. BMC Syst. Biol. 2, 17, 17.
Olszewski, M.M., Williams, C., Dong, K.C., Martin, A., 2019. The Cdc48 unfoldase prepares well-folded protein substrates for degradation by the 26S proteasome. Commun. Biol. 2, 29.
Orlandi, I., Ronzulli, R., Casatta, N., Vai, M., 2013. Ethanol and acetate acting as carbon/Energy sources negatively affect yeast chronological aging. Oxid. Med. Cell. Longev. 2013, 802870.
Peng, R.W., Guetg, C., Tigges, M., Fussenegger, M., 2010. The vesicle-trafficking protein munc18b increases the secretory capacity of mammalian cells. Metab. Eng. 12, 18–25.
Perez-Riverol, Y., Csordas, A., Bai, J., Bernal-Llinares, M., Hewapathirana, S., Kundu, D. J., Inuganti, A., Griss, J., Mayer, G., Eisenacher, M., Pérez, E., Uszkoreit, J., Pfeuffer, J., Sachsenberg, T., Yilmaz, S., Tiwary, S., Cox, J., Audain, E., Walzer, M., Jarnuczak, A.F., Ternent, T., Brazma, A., Vizcaíno, J.A., 2019. The PRIDE database and related tools and resources in 2019: improving support for quantification data. Nucleic Acids Res. 47, D442–d450.
Pham, P.V., 2018. Chapter 19 - medical biotechnology: techniques and applications. In: Barh, D., Azevedo, V. (Eds.), OMICS. Academic Press, pp. 449–469.
Protchenko, O., Philpott, C.C., 2003. Regulation of intracellular heme levels by *HMX1*, a homologue of heme oxygenase, in *Saccharomyces cerevisiae*. J. Biol. Chem. 278, 36582–36587.
Quintela-Carvalho, G., Luz, N.F., Celes, F.S., Zanette, D.L., Andrade, D., Menezes, D., Tavares, N.M., Brodskyn, C.I., Prates, D.B., Gonçalves, M.S., de Oliveira, C.I., Almeida, R.P., Bozza, M.T., Andrade, B.B., Borges, V.M., 2017. Heme drives oxidative stress-associated cell death in human neutrophils infected with Leishmania infantum. Front. Immunol. 8.
Rodnina, M.V., 2016. The ribosome in action: tuning of translational efficiency and protein folding. Protein Sci. 25, 1390–1406.
Ron, D., Walter, P., 2007. Signal integration in the endoplasmic reticulum unfolded protein response. Nat. Rev. Mol. Cell Biol. 8, 519–529.
Sánchez, B.J., Zhang, C., Nilsson, A., Lahtvee, P.-J., Kerkhoven, E.J., Nielsen, J., 2017. Improving the phenotype predictions of a yeast genome-scale metabolic model by incorporating enzymatic constraints. Mol. Syst. Biol. 13, 935.
Schuck, S., Prinz, W.A., Thorn, K.S., Voss, C., Walter, P., 2009. Membrane expansion alleviates endoplasmic reticulum stress independently of the unfolded protein response. J. Cell Biol. 187, 525–536.
Schwank, S., Ebbert, R., Rautenstrauss, K., Schweizer, E., Schüller, H.J., 1995. Yeast transcriptional activator INO2 interacts as an Ino2p/Ino4p basic helix-loop-helix heteromeric complex with the inositol/choline-responsive element necessary for expression of phospholipid biosynthetic genes in *Saccharomyces cerevisiae*. Nucleic Acids Res. 23, 230–237.
Semchyshyn, H.M., Abrat, O.B., Miedzobrodzki, J., Inoue, Y., Lushchak, V.I., 2011. Acetate but not propionate induces oxidative stress in bakers' yeast *Saccharomyces cerevisiae*. Redox Rep. 16, 15–23.
Séraphin, B., 1995. Sm and Sm-like proteins belong to a large family: identification of proteins of the U6 as well as the U1, U2, U4 and U5 snRNPs. EMBO J. 14, 2089–2098.
Solis-Escalante, D., Kuijpers, N.G., Barrajon-Simancas, N., van den Broek, M., Pronk, J.T., Daran, J.M., Daran-Lapujade, P., 2015. A minimal set of glycolytic genes reveals strong redundancies in *Saccharomyces cerevisiae* central metabolism. Eukaryot. Cell 14, 804–816.
Tripathi, N.K., Shrivastava, A., 2019. Recent developments in bioprocessing of recombinant proteins: expression hosts and process development. Front. Bioeng. Biotechnol. 7, 420, 420.
Tu, B.P., Ho-Schleyer, S.C., Travers, K.J., Weissman, J.S., 2000. Biochemical basis of oxidative protein folding in the endoplasmic reticulum. Science 290, 1571–1574.
Tu, B.P., Weissman, J.S., 2004. Oxidative protein folding in eukaryotes: mechanisms and consequences. J. Cell Biol. 164, 341–346.
Tyo, K.E., Liu, Z., Petranovic, D., Nielsen, J., 2012. Imbalance of heterologous protein folding and disulfide bond formation rates yields runaway oxidative stress. BMC Biol. 10, 16.
van Dijken, J.P., Bauer, J., Brambilla, L., Duboc, P., Francois, J.M., Gancedo, C., Giuseppin, M.L., Heijnen, J.J., Hoare, M., Lange, H.C., Madden, E.A., Niederberger, P., Nielsen, J., Parrou, J.L., Petit, T., Porro, D., Reuss, M., van Riel, N., Rizzi, M., Steensma, H.Y., Verrips, C.T., Vindeløv, J., Pronk, J.T., 2000. An interlaboratory comparison of physiological and genetic properties of four *Saccharomyces cerevisiae* strains. Enzym. Microb. Technol. 26, 706–714.
Vander Heiden, M.G., Cantley, L.C., Thompson, C.B., 2009. Understanding the Warburg effect: the metabolic requirements of cell proliferation. Science 324, 1029–1033.
Vieira Gomes, A.M., Souza Carmo, T., Silva Carvalho, L., Mendonça Bahia, F., Parachin, N.S., 2018. Comparison of yeasts as hosts for recombinant protein production. Microorganisms 6, 38.
Walsh, G., 2018. Biopharmaceutical benchmarks 2018. Nat. Biotechnol. 36, 1136–1145.
Wang, Y., Li, X., Chen, X., Nielsen, J., Petranovic, D., Siewers, V., 2021. Expression of antibody fragments in *Saccharomyces cerevisiae* strains evolved for enhanced protein secretion. Microb. Cell Factories 20, 134.
Wittrup, K.D., Benig, V., 1994. Optimization of amino acid supplements for heterologous protein secretion in *Saccharomyces cerevisiae*. Biotechnol. Tech. 8, 161–166.
Wolozin, B., Ivanov, P., 2019. Stress granules and neurodegeneration. Nat. Rev. Neurosci. 20, 649–666.
Zhan, C., Bidkhori, G., Schwarz, H., Malm, M., Mebrahtu, A., Field, R., Sellick, C., Hatton, D., Varley, P., Mardinoglu, A., Rockberg, J., Chotteau, V., 2020. Low shear stress increases recombinant protein production and high shear stress increases apoptosis in human cells. iScience 23, 101653.
Zhang, T., Bu, P., Zeng, J., Vancura, A., 2017. Increased heme synthesis in yeast induces a metabolic switch from fermentation to respiration even under conditions of glucose repression. J. Biol. Chem. 292, 16942–16954.
Zhang, Y.Q., Rao, R., 2010. Beyond ergosterol: linking pH to antifungal mechanisms. Virulence 1, 551–554.